Jestr

Journal of Engineering Science and Technology Review 14 (3) (2021) 15 - 22

JOURNAL OF
Engineering Science and Technology Review

Research Article

www.jestr.org

Design of Extreme Learning Machine based LFC for Three Area Interconnected Power System

M. Suman[1,*], M. Venu Gopala Rao[2] and P. V. Ramana Rao[3]

[1]*VLITS, Vadlamudi.*
[2]*PVPSIT, Kanuru.*
[3]*ANUCET, Nagarjuna Nagar.*

Received 11 September 2020; Accepted 20 May 2021

Abstract

This paper presents a novel extreme learning machine neural network for the Load Frequency Control of the interconnected system. There will be variance in the frequency from the reference value when there is a difference between active power generation and load demand. Significant disturbances contributing to frequency fluctuations beyond the acceptable limits are changes in load demand and faults etc. Initially PID based LFC which is a traditional controller is used to bring back the frequency differences when a disturbance occurs. But these conventional controllers will only operate certain operating points, are very slow and, for nonlinear systems, less efficient. Artificial intelligent controllers such as neural network controllers trained by ELM and BPNN algorithms are designed to avoid vulnerabilities in the conventional controller. The test system can be considered as a three, two and single area systems. All test systems' response is observed with and without PI, BPNN, and ELM neural network controllers. The ELM neural network controller is outperforming in damping the frequency variance due to the disturbances.

Keywords: Automatic Speed Governor, Back propagation algorithm, ELM algorithm, PI-Controller, Tie line, LFC.

1. Introduction

Today's electric power system incorporates several areas interconnected by tie line. In the electrical industry, LFC[1-3] is a major concern, and the power network must maintain system frequency and inter-area tie-line control fairly close to the accepted value for stable, high-quality electric power. By adjusting the mechanical input of the plant generator the frequency can be maintained at the reference value. Regardless of the disturbance that happens at any moment, such as the load fluctuations and faults, the frequency will be diverted from its rated value. The design of the power system has been that the network frequency and voltage need to be kept within tolerable limits. The main objective of any interconnected power system[4-5] does not only ensure good control of the frequency but also tieline power Several methods have been suggested for LFC. Although traditional control techniques have been employed in most research, as described in the literature, novel and intelligent control techniques have been used in several studies.

S. Kayalvizhi, D. M. Vinod Kumar [6] (2017) developed an adaptive fuzzy controller to control the load frequency with a Model Predictive Control. The test system is depicted as a single area network with an insulated microgrid, and the MPC controller's mathematical model is provided. The device response has been observed with and without PI, MPC, and Fuzzy MPC controllers, And it was observed that the proposed controller provides better performance in minimizing the ITSE. With the help of power reserve limitations, Le Thi Minh Trang and Hassan Nouri [7] (2018) model a dynamic load frequency controller. Current power networks will use the three separate reserves as reserves for repair, reserves for restore and reserves for containment. If there is a disruption inactive power generation and demand, a power reserve must be built to put back the state of equilibrium. In this paper the containment reserve is used to counteract the frequency variations due to disturbance.

Farag K. Abo-Elyousr and Adel M. Sharaf [8] (2019) have suggested a modern and reliable load frequency management system for the disturbances. With Distributed Energy Resource (DER) the PI controller is fractional-order used to counteract the variability in frequency. The test system is called two region control system. The device response was observed with phase disruption of 0.01 per p.u. Compared with the fractional-order PI system, the new approach is doing well.

S. Manikandan and Priyanka Kokil [9] (2019) given a time-variating load frequency controller dependent on delay to dampen the frequency variability due to disturbances. The study of the functionalities of Lyapunov and Krasovskii is used to find system stability. The test systems are called single field and two area frequency controllers. The Kp and Ki values are calculated to dampen the frequency differences concerning the delay range.

A load frequency controller was discussed by Diambomba Hyacinthe Tungadio and Yanxia Sun[10] considering the integration of renewable sources into the existing power network. The LFC controller is used to control the frequency of load and power in the tieline, whatever the sources it may be. LFC control operation with the PI controller and various methods of optimization of PI controller parameters. Clearly illustrate the fallbacks in the PI controller and the need for artificial smart powered controllers.

M.Suman et al. [11] (2019) designed an ELM power-dependent SVC FACTS controller to enhance the voltage at

*E-mail address: _machavarapu.suman@gmail.com
ISSN: 1791-2377
doi:10.25103/jestr.143.02

buses when there is a disturbance. Standard IEEE 30 and 5 bus systems are deemed the test systems. The parameters of the SVC FACTS controller are predicted via artificial neural networks. To train the neural network, two different algorithms are used, such as the Backpropagation and Extreme learning algorithms. The ELM algorithm efficiently and rapidly predicts the parameters. Three, two, and single area systems are considered as test systems. A step interruption of 0.01 p.u is managed to create, and the response of all three test systems is observed with and without various controllers.

2. Necessity of Keeping Frequency Constant

The exact reasons why system frequency changes [12] are kept to strict limits are as follows

- The speed of the AC motors is dependent on the frequency. The frequency change contributes to variations in motor speed
- The variable speed results in the display of incorrect time in electric clocks as they are driven by a synchronous motor.
- The turbines that operate with a frequency above the allowable limits can cause damage to the turbine blades.
- Network operation at the sub-normal voltage and frequency results in a revenue loss for the manufacturers due to the resulting drop in loads.
- The network frequency must be maintained constant so that the power stations run smoothly in parallel
- The operation of the power system is better monitored if the frequency deviation is implied by strict limits
- Changing frequency causes changes in consumer plant speed impacting manufacturing processes.

3. Mathematical modeling of single-area power system

Modeling the single area power network comprises of modeling [13-14] the speed governer, turbine, and generator load model. The speed governer's governing equations are as given in Equations 1 & 2.

$$\Delta y_{.E}(s) = \frac{k_{.1}*k_{.3}*k_C*\Delta P_{C.}(s) - k_2*k_{3.}*\Delta F(.s)}{k_4 + \frac{s}{k_5}} \quad (1)$$

Rearranging the Equation1, Equation 2 will be obtained

$$\Delta . Y_E(.s) = [\Delta P_{C.}(s) - \frac{1}{R} * \Delta F(s.)] * \frac{K_{sg.}}{1+T_{sg.}} \quad (2)$$

Where,

$R = \frac{k_1*k_c}{k_2}$ = Speed governor speed regulation

$K_{sg} = \frac{k_1*k_3*k_c}{k_4}$ = Speed governor gain

$T_{sg} = \frac{1}{k_4*k_5}$= Speed governor speed constant

Using Equation 2 the block diagram of the speed governor will be developed as shown in Figure 1.

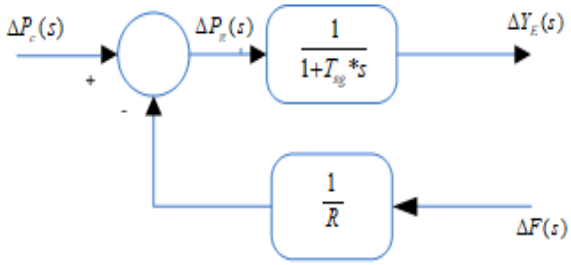

Fig. 1. Speed Governor block diagram

The mathematical equations and the block diagram of the turbine is as given in Equation 3 and Figure 2

$$\Delta P_t(s) = \frac{1}{1+T_t*s} * \Delta Y_e(s) \quad (3)$$

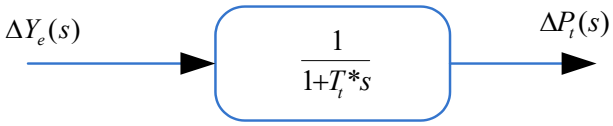

Fig. 2. Turbine block diagram

The equations governing the generator load model are given in Equation 4 & 5.

$$\Delta F(.s) = \frac{\Delta P_{g.}(s) - \Delta P_{d.}(s)}{B + \frac{2H}{f^0}*s} \quad (4)$$

Equation 4 can be rearranged as Equation 5

$$\Delta F(.s) = (\Delta P_{g.}(s) - \Delta P_{d.}(s)) * \frac{K_{ps.}}{1+T_{ps.}*s} \quad (5)$$

Where $T_{ps} = \frac{2*H}{B*f^0}$ = Time constant of power system

$Kps. = \frac{1}{B}$ = Gain of power system

The Generator Load model block diagram is represented as given in Figure 3.

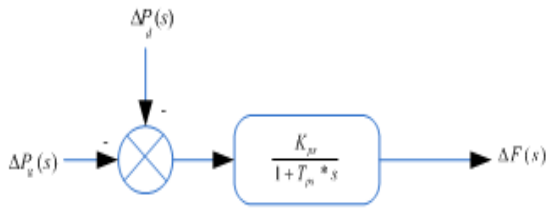

Fig. 3. Generator Load Model block diagram

The block diagram of the single area power network can be formed by combining the block diagrams of the speed governor, turbine, and generator load. The full block diagram with a feedback loop is shown in Figure 4.

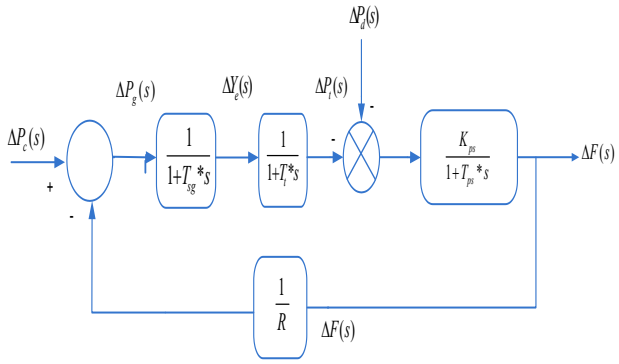

Fig. 4. Single area power network block diagram representation

4. Multi-Area Load Frequency Control

A Multi-area system can be formed by interconnecting different control areas. Two different areas interconnected by the tie line is given by given by Figure 5

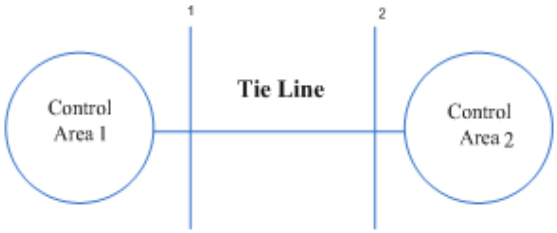

Fig. 5. Interconnection of two areas with tieline

In multi-area control the goal of the controller is to control the frequency of individual area as well as the tie line power. All the parameters correspond to the first area are represented with suffix 1 and the second area parameters are represented with suffix 2.

The equations governing the two area network is as given in Equations 6,7, 8,9 and 10.

$$\Delta F_{1.}(s) = [\Delta P_{g1.}(s) - \Delta P_{d1.}(s) - \Delta P_{tie1}(s)] * \frac{K_{ps1}}{1+T_{ps1}} \quad (6)$$

$$\Delta F_{2}(s) = [\Delta P_{g2.}(s) - \Delta P_{d2.}(s) - \Delta P_{tie2}(s)] * \frac{K_{ps2}}{1+T_{ps2}} \quad (7)$$

Let $K_{ps1} = \frac{1}{B1}$ and $T_{ps1} = \frac{2H_1}{B_1 * f}$

Also $\Delta P_{tie1} = \frac{2\Pi T_{12.}}{s}[\Delta F_{1.}(s) - \Delta F_{2.}(s)]$ (8)

$$\Delta P_{tie2} = -\frac{2\Pi a_{12.} T_{12.}}{s}[\Delta F_{1.}(s) - \Delta F_{2.}(s)] \quad (9)$$

The steady-state error in the tie-line power can be minimized using the PI controller. The area control errors for the two areas can be calculated as given in Equation.10

$$ACE_1(s) = \Delta P_{tie1}(s) + b_1 \Delta F_1(s) \quad (10)$$

$$ACE_2(s) = \Delta P_{tie2}(s) + b_2 \Delta F_2(s) \quad (11)$$

The basic concept of the three Area LFC and its block diagram is as given in Figure 6.

Rarely has the device of a single generator feeding a large and complex area existed in actual life. Many Parallel connected generators may be at a single location, or the load demand of such a wide area would be met at different locations. Wide load areas are split into several small areas, and the interconnected power systems satisfy the load demand accordingly. Power transfer between two areas is done via tie lines.

5. Artificial Neural Network controller

The ANNs [15-17] were designed primarily to mimic biological neural networks. ANN 's common [15,16] architectures are single, multi-layer, and feedback neural networks. The backpropagation algorithm is used mainly to train the neural networks of multilayer and feedforward. To obtain the optimized weights it makes use of the slow gradient descent process. The error is the difference between the actual output and the expected output. The generalized delta learning rule or the law of backpropagation is used to adjust the weights in such a way as to eliminate squared error and the actual output is about equal to the expected output. The weights are set according to. The diagram of the back propagation neural network as given in Figure 7.

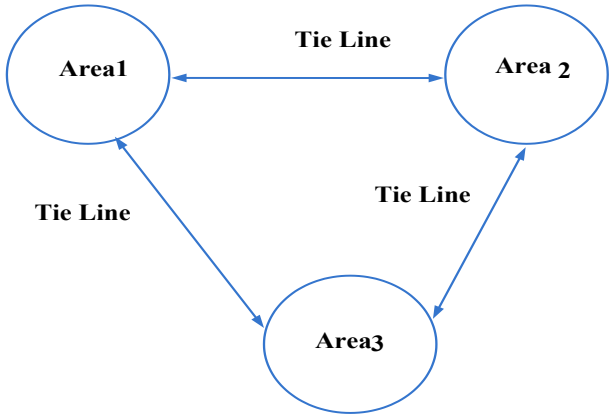

Fig. 6. Three Area inter Connection

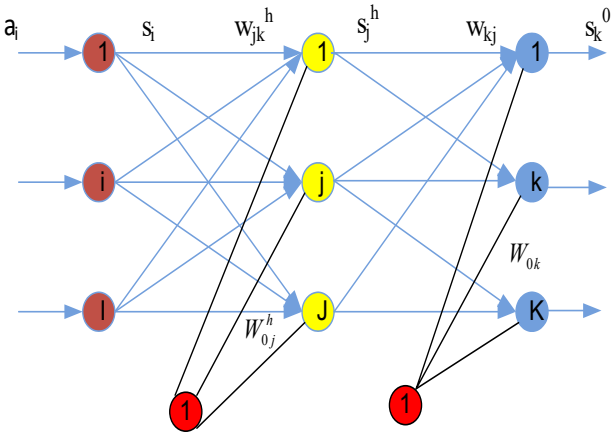

Fig.7 Multi-layer Feedforward Neural Network

The Multi-layer network consists of three layers as the input layer contains I number of neurons, one hidden layer contains J number of neurons, and the output layer contains the number of neurons k. The BPNN algorithm is as provided below

Step1. Provide inputs (a_i) and outputs (b_i) patterns.

Step2. Assume that only one hidden layer and initial weight setting are arbitrary, and make a = a(m)=a_l and b = b(m)=b_l.

Step3. Set the input layer unit i activation value to the x_i=a_i(m)

Step4. The j^{th} Neuron Activation value of hidden layer is calculated as

$$x_j^h = \sum_{i=1}^{I} w_j^k \, x_i + w_{oj}^h \tag{12}$$

Step5. The j^{th} unit output of the hidden layer is calculated as,

$$s_j^h = f_j^h(x_j^h) \tag{13}$$

Step6. The k^{th} unit activation value of the output layer,

$$x_k^0 = \sum_{i=1}^{I} w_{kj} \, x_j^h + w_{ok} \tag{14}$$

Step7. The output of the k^{th} neuron in the output layer,

$$s_k^0 = f_k^0(x_k^0) \tag{15}$$

Step8. The k^{th} output unit error term

$$\delta_k^0 = (b_k - s_k^0) * \dot{f}_k^0 \tag{16}$$

Step9. The weights between hidden and output layers can be calculated as,

$$w_{kj}(m+1) = w_{kj}(m) + \eta \delta_k^0 s_j^h \tag{17}$$

Step10. The Error term at the j^{th} hidden unit is calculated as

$$\delta_j^h = \dot{f}_j^h \sum_{k=1}^{K} \delta_k^0 \, w_{kj} \tag{18}$$

Step11. The weights between input and hidden layer can be updated as,

$$w_{ji}^h(m+1) = w_{ji}^h(m) + \eta \delta_j^h a_i \tag{19}$$

Step12. The error for the l^{th} pattern can be calculated as

$E_{l.} = \frac{1}{2}\sum_{k=1}^{K.}(b_{lk.} - s_k^{0.})^2$ and total error calculates as

$$E = \sum_{l=1.}^{L.} E_l \tag{20}$$

Step13. All the patterns are applied one by one and the weights are changed till the error is minimized.

The Backpropagation algorithm has some disadvantages as given below

- If the learning rate is selected small it converges slowly and became unstable if chosen high.
- It is agonizing with the problem of local minima.
- Sometimes ANNs are over-trained so that the algorithm may provide poor performance in generalization.
- In most applications gradient-based algorithms consume more time.

6. ELM Algorithm

When implementing an ELM Algorithm [18-20], the bottlenecks in the BPNN Algorithm are solved. ELM architecture comprises of input, single hidden and output layer. The input weights will be randomly generated and the output weights will be determined analytically.

By mathematics:

Let x_i be the inputs and y_i be the expected outputs where i=1: N. N is the number of patterns. The mathematical equations of the ELM network with h number of hidden layer neurons are as given in Equation.21.

$$Y(x_{k.}) = \sum_{i=1.}^{h} C_i \, G(x_i . a_k + b_i), k = 1.,2.,\ldots . N \tag{21}$$

Where C is the output weight matrix, a_k is the input weight matrix and the bias weight matrix is b .

The architecture of the ELM network could be seen as illustrated in Figure 8.

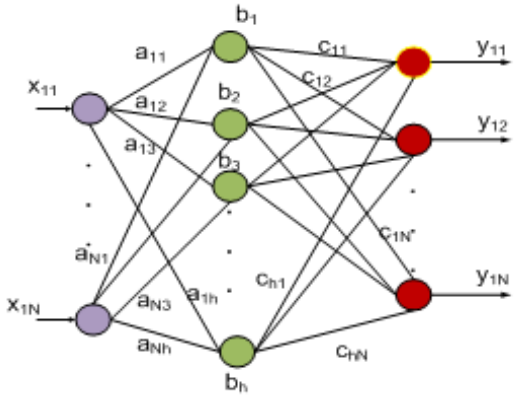

Fig. 8. The architecture of the ELM network

In matrix notation the Eqn . (17) can be written as:

$$G^* C = Y \tag{22}$$

G is a matrix of hidden-layer output and Y is a matrix of ELM output .

$$\begin{bmatrix} g(a_1 * x_1 + b_1) & \circ & \circ & g(a_n * x_1 + b_n) \\ \circ & \circ & \circ & \circ \\ \circ & \circ & \circ & \circ \\ g(a_1 * x_n + b_1) & & & g(a_n * x_n + b_n \end{bmatrix} \tag{23}$$

$$\beta = \begin{bmatrix} C_1^T \\ \circ \\ \circ \\ C_n^T \end{bmatrix} \qquad Y = \begin{bmatrix} y_1^T \\ \circ \\ \circ \\ y_n^T \end{bmatrix} \tag{24}$$

This can be compared in a gradient-based backpropagation algorithm similar to cost function minimization.

$$F_{BP} = \sum_{i=1}^{N} \left[\sum_{j=1}^{h} \beta_j \, G(x_i . a_j + b_i) - y_i \right] \tag{25}$$

The output weight matrix elements shall be determined with randomly assigned input weights and biases

$$C = G^{+} * Y \tag{26}$$

The matrix G^{+} is the Moore – Penrose inverse of matrix G,

Simply the algorithm of the ELM for this particular problem can be written as follows

Step 1: The variation of frequency concerning step disturbance is provided as input to the network.

Step 2: The Input weights and biases are randomly generated and the output weights are calculated analytically.

Step 3: With input and output weights, the output of the network is determined.

Step 4: With the output provided by the ELM LFC controller quickly the deviation in frequency will be damped.

The ELM has numerous assets such as high-speed learning, good generalization efficiency, usage of non-differential activation function, the over fitting problem is avoided, local minima problem also minimized, and imprecision in learning compared to classical learning techniques.

7. Simulation results

The deviation in frequency of the single area system was observed without and with PI, fuzzy, and neural network controllers. The single area Load frequency control with the BPNN is as given in Figure 9.

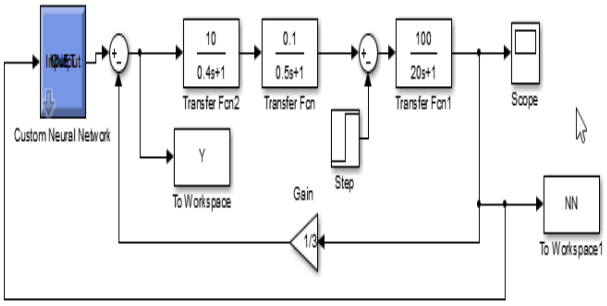

Fig..9 Simulation diagram of BPNN LFC

The simulation diagram of the ELM LFC is as given in Figure.10

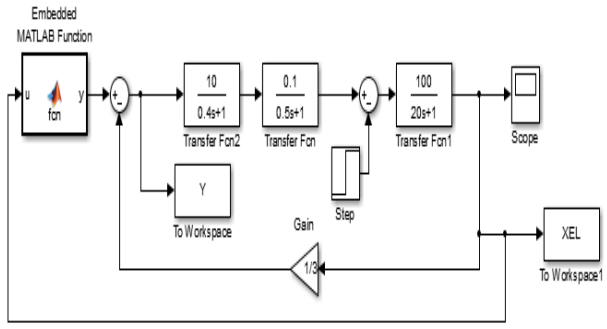

Fig..10 Simulation diagram of ELM LFC

The deviation in frequency of the single area system without and with different controllers is as given in Figure.11 to Figure.14.

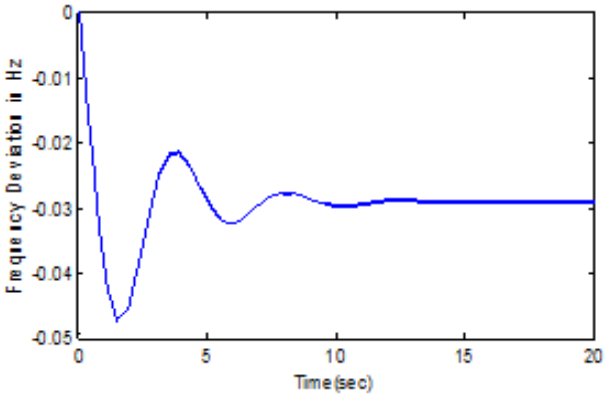

Fig.11 Single area LFC without the controller

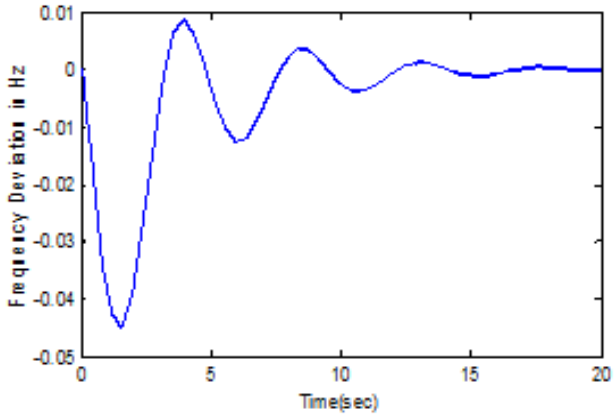

Fig.12 Single area LFC with PI controller

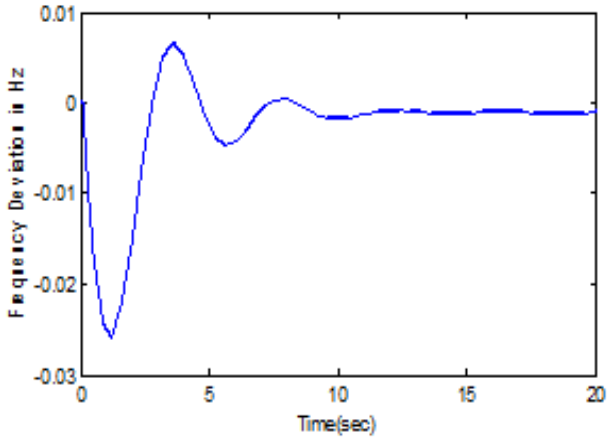

Fig..13 Single are LFC with the Backpropagation neural network controller

The comparison table of peak values and settling times of the single area system is as given in Table.1

The performance of different controllers observed with two area test systems also. The Figures15 to 18 shows the response of different controllers.

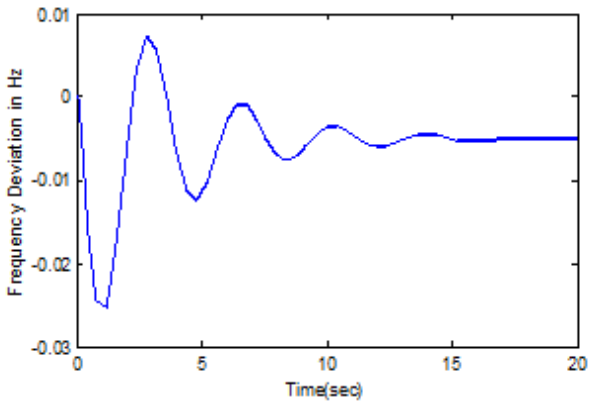

Fig.14 Single are LFC with the ELM neural network controller

Table.1 Comparision of performance of controllers on a single area

S.No	Controller	Peak Overshoot	Settling time
1	Without	-0.0475	Never settles at zero
2	PI	-0.045	27
3	BPNN	-0.0265	15.8
4	ELMNN	-0.025	15.5

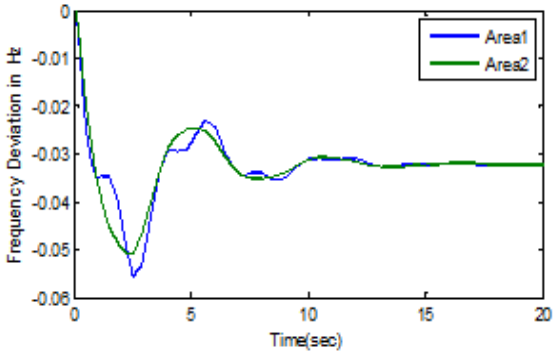

Fig.15 Two area LFC without the controller

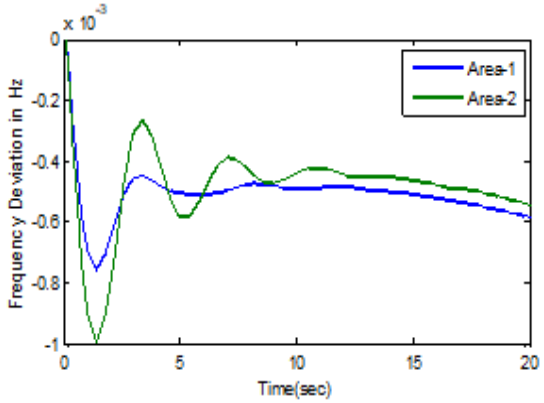

Fig.16 Two area LFC with PI controller

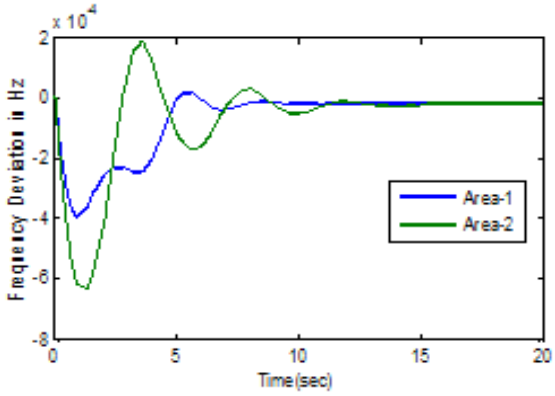

Fig.17 Two area LFC with the Backpropagation neural network controller

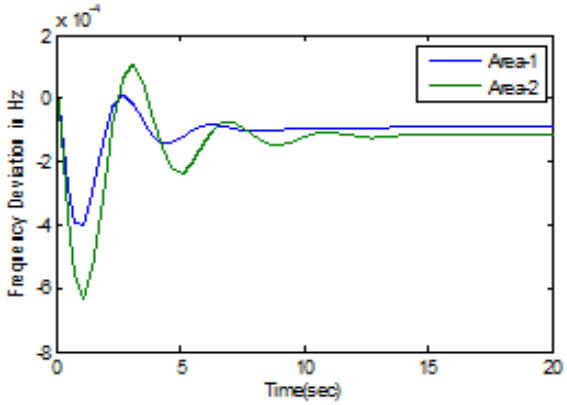

Fig.18 Single are LFC with the ELM neural network controller

The performance comparison of different controllers of two are system is given in Table.2

The three area test system response also observed with the different controllers which are given in Figure.19 to 22.

Table.2. Comparison of performance of controllers on Two area

Area	Controller	Peak Overshoot	Settling time
1	Without	-0.055	Never settles at zero
	PI	-0.0007	26
	BPNN	-0.0004	16.5
	ELMNN	0.00038	15.4
2	Without	-0.051	Never settles at zero
	PI	-0.001	26.5
	BPNN	0.00063	16
	ELMNN	0.00061	15

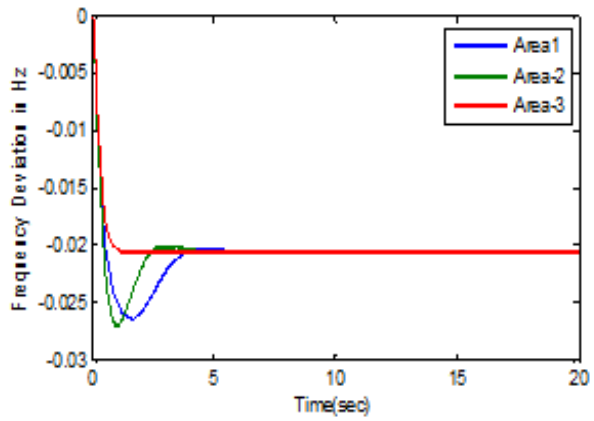

Fig.19 Two area LFC without the controller

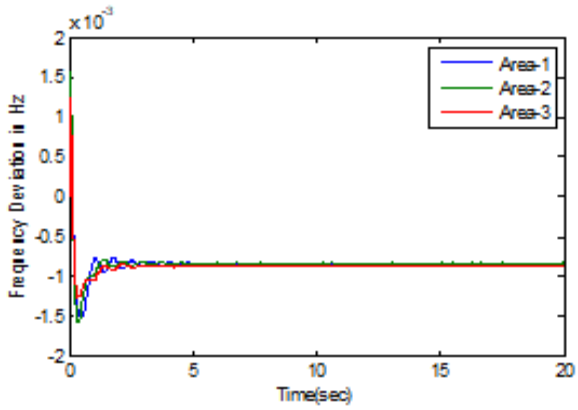

Fig.21 Two area LFC with the Backpropagation neural network controller

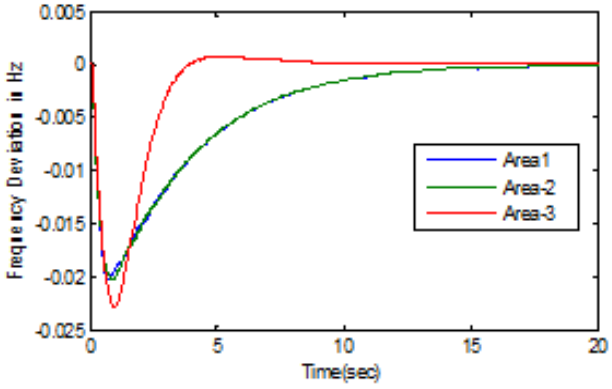

Fig.20 Two area LFC with PI controller

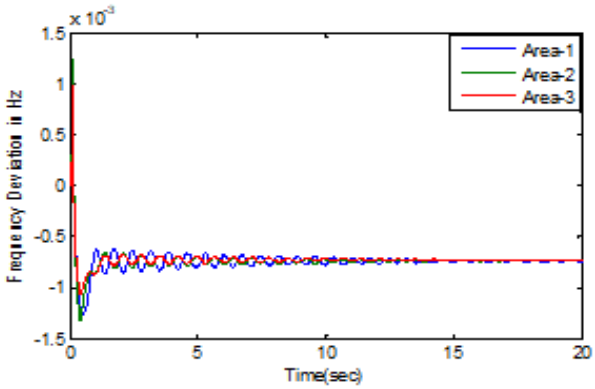

Fig.22 Single are LFC with the ELM neural network controller

Table.3. Comparison of performance of controllers on Two area

Area	Controller	Peak Overshoot	Settling time
1	Without	-0.027	Never settled to zero
	PI	-0.019	31
	BPNN	-0.015	9.8
	ELMNN	-0.011	9.5
2	Without	-0.0275	Never settled to zero
	PI	-0.02	30.5
	BPNN	-0.0155	9.2
	ELMNN	-0.0125	9.1
3	Without	-0.026	Never settled to zero
	PI	-0.024	30.1
	BPNN	-0.0165	8.2
	ELMNN	-0.013	8

The performance comparison of different controllers of two are system is given in Table.3

8. Conclusion:

The frequency deviation was observed with a step disturbance of 0.01 p.u for a single area, two area and three area interconnected power systems, without and with PI, Fuzzy, and Neural network controller. The peak value and the settling time for different test systems were observed with all the controllers. Consider, for example, the single area system without the LFC controller the peak value will be -0.045 Hz and it will not settle back to null. The PI controller can bring the peak value back to -0.045 Hz and the settling time to 27 sec. The fuzzy controller will control the peak value at -0.027 Hz and the 17.5 sec settling time. For the extreme learning machine algorithm, the peak value and the settling time will be -0.025 Hz and 15.5 sec. The controller to controler the response is improving in the single area system and the ELM based neural network controller provides the best performance. Like this, the proposed system is outperforming

in the remaining two area and three area systems as compared to the remaining controller.

References

1. Ranganayakulu, R., Babu, G.U., Rao, A.S., Patle, D.S.: A comparative study of fractional order PI/PID tuning rules for stable first order plus time delay processes. Resour. Eff. Tech. 2, 136–152 (2016)
2. Anil Annamraju, Srikanth Nandiraju"Robust frequency control in a renewable penetrated power system: an adaptive fractional order-fuzzy approach" Protection and Control of Modern Power Systems, Vol.4, Isuue.16, 2019.
3. Liu, H., Hu, Z., Song, Y., et al. (2015). Vehicle-to-grid control for supplementary frequency regulation considering charging demands. IEEE Transactions on Power Systems, 30(6), 3110–3119.
4. Debbarma, S., & Dutta, A. (2017). Utilizing electric vehicles for LFC in restructured power systems using fractional order controller. IEEE Transactions on Smart Grid, 8(6), 2554–2564.
5. Sandeep Hanwate, Yogesh V. Hote, "Adaptive Policy for Load Frequency Control" IEEE Transactions on Power Systems, Volume: 33 , Issue: 1 , pp. 1142 - 1144Jan. 2018
6. S. Kayalvizhi, D. M. Vinod Kumar, "Load Frequency Control of an Isolated Micro grid using Fuzzy Adaptive Model Predictive control" IEEE Access, Vol.5, pp. 16241 – 16251, 14 August 2017.
7. Le Thi Minh Trang, "Modeling Dynamic Frequency Control with Power Reserve Lmitations" 53rd International Universities Power Engineering Conference,sep.,2018
8. T3. Farag K. Abo-Elyousr, Adel M. Sharaf "A novel modified robust load frequency controller scheme" Energy Systems, 05 June 2019.
9. S. Manikandan and Priyanka Kokil, "Delay-Dependent Stability Analysis of Network-Based Load Frequency Control of One and Two Area Power System with Time-Varying Delays "Fluctuation and Noise Letters, Vol. 18, No. 1, pp.1 -19, 2019.
10. Abhijith Pappachen, A. Peer Fathima, "Critical research areas on load frequency control issues in a deregulated power system: A state-of-the-art-of-review" Renewable and Sustainable Energy Reviews, Vol.72, pp. 163–177, 2017.
11. M. Suman ; M. Venu Gopala Rao , P.V.Ramana Rao," Machine Learning Algorithm Based Static VAR Compensator to Enhance Voltage Stability of Multi-machine Power System", Mathematical Modelling of Engineering Problems,pp.641-649, 24 December 2019
12. M. Suman ; M. Venu Gopala Rao ; G.R.S Naga Kumar ; O. Chandra Sekhar" Load frequency control of three unit interconnected multimachine power system with PI and fuzzy controllers" 2014 International Conference on Advances in Electrical Engineering (ICAEE), 9-11 Jan. 2014.
13. Kamlesh Bharti, Vijay P. Singh ,S. P. Singh " Impact of Intelligent Demand Response for Load Frequency Control in Smart Grid Perspective" IETE Journal of Research, pp.1-12, 10 Jan 2020.
14. Surya Prakash, S. K. Sinha," Application of artificial intelligence in load frequency control of interconnected power system" International Journal of Engineering, Science and Technology, Vol. 3, No. 4, pp. 264-275, 2011
15. Deepak Kumar Lal, Ajit Kumar Barisal "Combined load frequency and terminal voltage ontrol of power systems using moth flame optimization algorithm" Journal of Electrical Systems and Information Technology, Vol.6,No.8, 00.1-24, 2019.
16. 14. D. Khamari, J. K.Rout, " Load Frequency Control of two Area Power System using PID1 Controller" International Journal of Engineering Research & Technology (IJERT), pp.245-248, Vol. 8 Issue 03, March-2019
17. Diambomba Hyacinthe Tungadio, Yanxia Sun, "Load frequency controllers considering renewable energy integration in power system" Energy Reports 5 (2019) 436–454.
18. Hongfeng Li, HongkaiZhao,Hong Li,"Neural-Response-Based Extreme LearningMachine for Image Classification",IEEE Transactions on Neural Networks and Learning Systems, Vol.30, No.2,pp.539-552, Feb 2018
19. EnderSevinc,"A Novel Evolutionary Algorithm for DataClassification Problem With ExtremeLearning Machines", IEEE Access, Vol.7,pp.122419 – 122427, 2019 Can Wan , Zhao Xu , Pierre Pinson , Zhao Yang Dong ,Kit Po Wong,"Probabilistic Forecasting of Wind Power GenerationUsing Extreme Learning Machine",IEEE Transactions on Power Systems, Vol.29, No.3, pp.1033-1044, 2014